*Available online www.jocpr.com*

**Journal of Chemical and Pharmaceutical Research, 2015, 7(1):37-45**

**Research Article**

**ISSN : 0975-7384**
**CODEN(USA) : JCPRC5**

# Thermodynamic and interfacial studies on solid dispersions of phenothiazine-2-methylimidazole drug system

**Manoj Kumar and H. Shekhar**

*Department of Chemistry, V. K. S. University, Ara, India*

---

**ABSTRACT**

*The study of solid liquid dispersions of binary drug system has been very useful in providing the significant enhanced pharmaceutical properties as compared to the parent drug. The present communication includes the thermodynamic and interfacial investigation of phenothiazine (PT) and 2-methylimidazole (MIM) binary eutectic and non-eutectic drug dispersion. Simple eutectic dispersion was observed at 0.785 mole fraction of MIM at melting temperature 122 ℃. Partial and Integral thermodynamic quantities such as, excess Gibbs energy ($g^E$), excess enthalpy ($h^E$), excess entropy ($s^E$) of eutectic and non-eutectic mixtures were also calculated using activity coefficient data. The value of excess Gibbs free energy indicates positive deviation from ideal behaviour which refers stronger association between like molecules during formation of binary mix. However, the negative value of mixing function as Gibbs free energy of mixing ($\Delta G^M$) suggests the mixing for eutectic and non-eutectic is spontaneous. The interfacial properties such as entropy of fusion per unit volume ($\Delta S_V$), interfacial energy ($\sigma$), roughness parameter ($\alpha$), grain boundary energy of parent components, eutectics and non-eutectics have been studied using enthalpy of fusion data. Gibbs-Thomson coefficient evaluated by numerical method is also very helpful to compute the interfacial energy. The size of critical nucleus at different undercoolings has been found in nanoscale, which may lead a big challenge in pharmaceutical world. The value of $\alpha > 2$, suggests the irregular and faceted growth proceeds in binary alloys.*

**Keywords**: phase diagram, thermodynamic and mixing functions. Thermal stability, Critical radius, Interfacial energy and microstructure.

---

## INTRODUCTION

During last few years the solid dispersion drugs of binary pharmaceutical systems are being demonstrated as model system to improve solubility, maximize the therapeutic efficacy and make of value of drug. Wide application of these dispersions [1, 2] can also be understood to a great extent with the help of kinetic, themodynamic and interfacial investigation. Phenothiazines have gained much significant importance in the area of pharmaceutical applications [3-5]. The scientific and medical interests of phenothiazines have been considered as multidrug-resistant mycrobacterium, tuberculosis (MDRTB) [6, 7], plasmid-antibiotic- resistant genes [8] and Methicillin-resistant staphytococus aureus (MRSA) which are the major global lethal and noscomial infection and are responsible for over 4 million deaths per year. The mild neuroleptic action of PT as compared to their equivalent compounds has got much credit for the management of these infections. The activity of PTs against protozoa, parasites, antimicrobial effects and their potential for the therapy of stated problematic infections have also been highlighted earlier. Phenothiazines inhibit ABC type efflus pumps that respond for the antibiotic resistance of many micro-organisms [9]. They also inhibit calcium binding to calmodulion type proteins of the calcium channel verapamil. On the other hand 2-methylimidazole is an important class of heterocyclic compounds which show diverse types of biological and pharmacological properties. Imidazole nucleus has proved to be an abundant source for a number of medicinal agents and associated with many activities. Several derivatives of imidazoles have been reported as antagonists [10], antiprotozoal, mutagenic properties, anticancer, antiviral, muscarinic anticholingergic

activity enzyme inhibition, H2-Antagonism, α-Adrenergic agonist and β-blocking, anticonvulsant, broad spectrum antibacterial, antispasmodic activity and antifungal activities. The polar imidazoles, soluble in water are found potentially less toxic to human.

In view of diverse biological and pharmacological applications of phenothiazines and 2-methylimidazoles, they represent a good lead in developing and designing of virgin and new binary drugs. However, very little information is available with regard to binary drug materials of eutectic, non eutectic and additive types solid dispersions. In recent years pharmaceutical properties of some binary solid dispersion/co-crystals has been reported emphasizing the solubility, dissolution rate, hygroscopicity and chemical stability. Keeping the view of better pharmacological performance and efficacy of binary product, the present communication is aimed to investigate binary drug dispersions of phenothiazines (PT) and 2-methylimidazole (MIM) with emphasizing their thermodynamic and interfacial studies, such as phase diagram, excess and mixing thermodynamic functions, activity and activity coefficient, thermal stability, interfacial energy, surface roughness, driving force of solidification and critical radius.

## EXPERIMENTAL SECTION

Phenothiazines (PT) (Sigma, India) and 2-Methylimidazoles (MIM) were directly taken for investigation. The melting point of Phenothiazines was found 189°C while for 2-Methylimidazoles it was found 142°C. For measuring the solid-liquid equilibrium data of PT-MIM system, mixtures of different compositions of both were made in glass test tubes by repeated heating and followed by chilling in ice and melting temperatures of solid dispersions were determined by the thaw-melt method[11,12]. The melting and thaw temperatures were determined in a Toshniwal melting point apparatus using a precision thermometer which could read correctly up to ± 0.1°C. The heater was regulated to give above 1°C increase in temperature in every five minutes. The literature value[13] of enthalpy of fusion of Phenothiazines and 2-Methylimidazoles was used in determining the various thermodynamic parameters of the binary system.

## RESULTS AND DISCUSSION

### SLE Study

The solid liquid equilibrium (SLE) data of PT-MIM system determined by the thaw melt method is reported in Table 1. The system shows the formation of a eutectic (E) and non-eutectics solid dispersions (A1-A10). The melting point of PT (189°C) decreases on the addition of second component MIM (M.P., 142°C) and further attains minimum and then increases. Eutectic E (0.215 mole fraction of PT) is obtained at 122°C. At the eutectic temperature a liquid phase L and two solid phases ($S_1$ and $S_2$) are in equilibrium and the system is invariant. The homogenous binary liquid solution exists in the region above the eutectic temperature while the two solid phases exists in the region below the eutectic temperature. The region located below the liquidus line on the left side a binary liquid and solid PT exist while in a similar region located on the right side a binary liquid and solid MIM system co-exist.

$$L \underset{}{\overset{\text{Cooling}}{\rightleftharpoons}} S_1 + S_2$$

### Thermodynamic Study

The values of heats of fusion of eutectic and non-eutectic are calculated by the mixture law. The value of heat of fusion of binary solid dispersions $A_1$-$A_{10}$ and E is reported in Table 1. The activity coefficient and activity of components for the systems under investigation has been calculated from the equation[14] given below

$$-\ln \chi_i \gamma_i = \frac{\Delta H_i}{R}\left(\frac{1}{T_e} - \frac{1}{T_i}\right) \quad (1)$$

where $\chi_i, \gamma_i$ is mole fraction and activity coefficient of the component *i* in the liquid phase respectively. $\Delta H_i$ is the heat of fusion of component i at its melting point $T_i$ and R is the gas constant. $T_e$ is the melting temperature of alloy. Using the values of activity and activity coefficient of the components in the binary product, the mixing and excess thermodynamic functions have been evaluated.

**Mixing Functions**

In order to know the mixing characteristics of components in the system Integral molar free energy of mixing ($\Delta G^M$), molar entropy of mixing ($\Delta S^M$) and molar enthalpy of mixing ($\Delta H^M$) and partial thermodynamic mixing functions of the binary solid dispersions were determined by using the following equations

$$\Delta G^M = RT\,(\chi_{PT}\, ln a_{PT} + \chi_{MIM}\, ln a_{MIM}) \quad (2)$$

$$\Delta S^M = -R\,(\chi_{PT}\, ln\chi_{PT} + \chi_{MIM}\, ln\chi_{MIM}) \quad (3)$$

$$\Delta H^M = RT\,(\chi_{PT}\, ln\gamma_{PT} + \chi_{MIM}\, ln\gamma_{MIM}) \quad (4)$$

$$\bar{G}_i^M = \bar{\mu}_i^M = RT\, ln a_i \quad (5)$$

where $\bar{G}_i^M$ ($\bar{\mu}_i^M$) is the partial molar free energy of mixing of component i (mixing chemical potential)in binary mix and $\gamma_i$ and $a_i$ is the activity coefficient and activity of component respectively. The negative value[15] of molar free energy of mixing of alloys (Table 2) suggests that the mixing in all cases is spontaneous. The integral molar enthalpy of mixing value corresponds to the value of excess integral molar free energy of the system favors the regularity in the binary solutions.

**Excess Functions**

In order to unfold the nature of the interactions between the components forming the eutectic and non-eutectic solid dispersions, the excess thermodynamic functions such as integral excess integral free energy ($g^E$), excess integral entropy ($s^E$) and excess integral enthalpy ($h^E$) were calculated using the following equations

$$g^E = RT(\chi_{PT} \ln\gamma_{PT} + \chi_{\mathrm{MIM}} \ln\gamma_{MIM}) \quad (6)$$

$$s^E = -R\left( (\chi_{PT} \ln\gamma_{PT} + \chi_{MIM} \ln\gamma_{MIM} + \chi_{PT} T \frac{\delta \ln\gamma_{PT}}{\delta T} + \chi_{MIM} T \frac{\delta \ln\gamma_{MIM}}{\delta T} \right) \quad (7)$$

$$h^E = -RT^2\left( \chi_{PT} \frac{\delta \ln\gamma_{PT}}{\delta T} + \chi_{MIM} \frac{\delta \ln\gamma_{MIM}}{\delta T} \right) \quad (8)$$

and excess chemical potential or excess partial free energy of mixing;

$$g_i^{-E} = \mu_i^{-M} = RT \ln\gamma_i \quad (9)$$

The values of $\delta \ln\gamma_i / \delta T$ can be determined by the slope of liquidus curve near the alloys. The values of the excess thermodynamic functions are given in Table 3. The value of the excess free energy is a measure of the departure of the system from ideal behaviour. The reported excess thermodynamic data substantiate the earlier conclusion of an appreciable interaction between the parent components during the formation of alloys. The positive $g^E$ value [16] for all eutectic and non-eutectic solid dispersions infers stronger interaction between like molecules in binary mix. The excess entropy is a measure of the change in configurational energy due to a change in potential energy and indicates an increase in randomness.

**Gibbs-Duhem Equation**

Further the partial molar quantity, activity and activity coefficient can also be determined by using Gibbs-Duhem equation

$$\sum \chi_i dz_i^{-M} = 0 \quad (10)$$

$$or \quad \chi_{PT} dH_{PT}^{-M} + \chi_{MIM} dH_{MIM}^{-M} = 0 \quad (11)$$

$$or \quad dH_{PT}^{-M} = \frac{\chi_{MIM}}{\chi_{PT}} dH_{MIM}^{-M} \quad (12)$$

$$or \quad [H_{PT}^{-M}]_{x_{PT}=y} = \int_{\chi_{PT}=y}^{\chi_{PT}=1} \frac{\chi_{MIM}}{\chi_{PT}} dH_{MIM}^{-M} \tag{13}$$

Graph between $H_{MIM}^{-M}$ and $\chi_{MIM}/\chi_{PT}$ gives the solution of the partial molar heat of mixing of a constituent PT in binary mix and plot between $\chi_{MIM}/\chi_{PT}$ vs $\ln a_{MIM}$ determines the value of activity of component PT in binary mix.

**Stability Function**

Thermodynamic behaviour of the present system in form of stability and excess stability functions [17] can be determined by the second derivative of their molar free energy and excess energy respectively, with respect to the mole fraction of either constituent:

$$Stability = \frac{\partial^2 \Delta G^M}{\partial x^2} = -2RT \frac{\partial \ln a}{\partial (1-x)^2} \tag{14}$$

$$Excess \;\; Stability = \frac{\partial^2 g^E}{\partial x^2} = -2RT \frac{\partial \ln \gamma}{\partial (1-x)^2} \tag{15}$$

These values were calculated by multiplying the slope of lna vs $(1 – x)^2$ and lnγ vs $(1 – x)^2$ plots with -2RT. The best polynomial equation of the curve generated is given as:

$$\ln \gamma = 3.68(1-x)^2 - 21.44(1-x)^4 + 81.99(1-x)^6 - 146.84(1-x)^8 + 126.(1-x)^{10} - 41.47(1-x)^{12} \tag{16}$$

The slope of the curve shown in figure as obtained by differentiating the above equation with respect to $(1 – x)^2$ may also be used to calculate the excess stability of the PT-MIM system. The values of total stability to the ideal stability and defined as

$$Ideal \;\; Stability = \frac{RT}{x(1-x)} \tag{17}$$

These values show there is considerable thermodynamic stability in the alloy. The (fig.2) for the stability, excess stability and ideal stability in the form of composition and partial Gibb's energy favours the formation of the binary dispersions and their mixing.

**Interfacial Investigation**

**The Solid-Liquid Interfacial Energy (σ)**

It has been realized that an experimentally observed value of interfacial energy 'σ' keeps a variation of 50-100% from one worker to other. However, Singh and Glickman [18] were calculated the solid-liquid interfacial energy ($\sigma$) from melting enthalpy change and values obtained are found in good agreement with the experimental values. Turnbull empirical relationship [19] between the interfacial energy and enthalpy change provides the clue to determine the interfacial energy value of binary solid dispersions and is expressed as:

$$\sigma = \frac{C\Delta H}{(N)^{1/3}(V_m)^{2/3}} \tag{18}$$

where the coefficient *C* lies between 0.33 to 0.35 for nonmetallic system, $V_m$ is molar volume and N is the Avogadro's constant. The value of the solid-liquid interfacial energy of phenothiazine and 2-methyimidazole was found to be $3.61 \times 10^{-2}$ and $2.60 \times 10^{-2}$ J $m^{-2}$ respectively and σ value of the solid dispersions was given in Table 1. The value of σ has also been determined by using the value of Gibbs-Thomson coefficient. The theoretical basis of determination of τ was made for equal thermal conductivities of solid and liquid phases for some transparent materials.

**Gibbs-Thomson Coefficient ($\tau$)**

For a planar grain boundary on planar solid-liquid interface the Gibbs-Thomson coefficient ($\tau$) for the system can be calculated by the Gibbs-Thomson equation and is expressed as

$$\tau = r\Delta T = \frac{TV_m\sigma}{\Delta H} = \frac{\sigma}{\Delta S_V} \quad (19)$$

where τ is the Gibbs-Thomson coefficient, ΔT is the dispersion in equilibrium temperature and, r is the radius of grooves of interface. It was also determined by the help of Gunduz and Hunt numerical method [20] for materials having known grain boundary shape, temperature gradient in solid and the ratio of thermal conductivity of the equilibrated liquid phases to solid phase ($R = K_L/K_S$).The Gibbs-Thomson coefficient for PT, MIM and their solid dispersions are found in the range of 7.07 – 9.51 x $10^6$ Km and is reported in Table 1.

**Interfacial Grain Boundary Energy ($\sigma_{gb}$)**

Grain boundary is the internal surface which can be understood in a very similar way to nucleation on surfaces in liquid-solid transformation. In past, a numerical method [21] is applied to observe the interfacial grain boundary energy ($\sigma_{gb}$) without applying the temperature gradient for the grain boundary groove shape. For isotropic interface there is no difference in the value of interfacial tension and interfacial energy. A considerable force is employed at the grain boundary groove in anisotropic interface. The grain boundary energy can be obtained by the equation:

$$\sigma_{gb} = 2\sigma \cos\theta \quad (20)$$

where θ is equilibrium contact angle precipitates at solid-liquid interface of grain boundary. The grain boundary energy could be twice the solid-liquid interfacial energy in the case where the contact angle tends to zero. The value of $\sigma_{gb}$ for solid PT and MIM was found to be 6.98 x $10^2$ and 5.03 x $10^2$ $Jm^{-2}$ respectively and the value for all solid dispersions is given in Table 1.

**The Effective Entropy Change ($\Delta S_v$)**

It is obvious that the effective entropy change and the volume fraction of phases in the alloy are inter-related to decide the interface morphology during solidification and the volume fraction of the two phases depends on the ratio of effective entropy change of the phases. The entropy of fusion (ΔS = ΔH/T) value (Table 1) of alloys is calculated by heat of fusion values of the materials. The effective entropy change per unit volume ($\Delta S_V$) is given by

$$\Delta S_V = \frac{\Delta H}{T}.\frac{1}{V_m} \quad (21)$$

where $\Delta H$ is the enthalpy change, T is the melting temperature and $V_m$ is the molar volume of solid phase. The entropy of fusion per unit volume ($\Delta S_V$) for PT and MIM was found 379 and 368 $kJK^{-1}m^{-3}$ respectively. Values of $\Delta S_V$ for alloys are reported in Table 1.

**The Driving Force of Nucleation ($\Delta G_v$)**

During growth of crystalline solid there is change in enthalpy, entropy and specific volume and non-equilibrium leads the Gibb's energy. Thermodynamically metastable phase occurs in a supersaturated or super-cooled liquid. The driving force for liquid-solid transition is the difference in Gibb's energy between the two phases. The theories of solidification process in past have been discussed on the basis of diffusion model, kinetic characteristics of nucleation and on thermodynamic features. The lateral motion of rudementry steps in liquid advances stepwise with non-uniform surface at low driving force while continuous and uniform surface advances at sufficiently high driving force. The driving force of nucleation from liquid to solid during solidification ($\Delta G_V$) can be determined at different undercoolings (ΔT) by using the following equation [22]

$$\Delta G_V = \Delta S_v \Delta T \quad (22)$$

It is opposed by the increase in surface free energy due to creation of a new solid-liquid interface. By assuming that solid phase nucleates as small spherical cluster of radius arising due to random motion of atoms within liquid. The value of $\Delta G_V$ for each solid dispersions and pure components are shown in the Table 4.

**The Critical Radius (r*)**

During liquid-solid transformation embryos are rapidly dispersed in unsaturated liquid and on undercooling liquid becomes saturated and provides embryo of a critical size with radius r* for nucleation which can be determined by the Chadwick relation [23]

$$r^* = \frac{2\sigma}{\Delta G_V} = \frac{2\sigma T}{\Delta H_V \Delta T} \tag{23}$$

where σ is the interfacial energy and $\Delta H_V$ is the enthalpy of fusion of the compound per unit volume, respectively. The critical size of the nucleus for the components and alloys was calculated at different undercoolings and values are presented in Table 5. It can be inferred from table that the size of the critical nucleus decreases with increase in the undercooling of the melt. The existence of embryo and a range of embryo size can be expected in the liquid at any temperature. The value of r* for pure components (PT and MIM) and solid dispersions lies between 40 to 190 nm at undercooling 1 – 3.5°C.

**Critical Free Energy of Nucleation (ΔG*)**

To form critical nucleus, it requires a localized activation/critical free energy of nucleation (ΔG*) which is evaluated [24] as

$$\Delta G^* = \frac{16}{3}\frac{\pi\sigma^3}{\Delta G_v^2} \tag{24}$$

The value of ΔG* for alloys and pure components has been found in the range of $10^{-16}$ J per molecule at different undercoolings, and has been reported in Table 6.

**Interface Morphology**

The science of growth has been developed on the foundation of thermodynamics, kinetics, fluid dynamics, crystal structures and interfacial sciences. The solid-liquid interface morphology can be predicted from the value of the entropy of fusion. According to Hunt and Jackson [25], the type of growth from a binary melt depends upon a factor α, defined as:

$$\alpha = \xi\frac{\Delta H}{RT} = \xi\frac{\Delta S}{R} \tag{25}$$

where $\xi$ is a crystallographic factor depending upon the geometry of the molecules and has a value less than or equal to one. ΔS/R (also known as Jackson's roughness parameter α) is the entropy of fusion (dimensionless) and R is the gas constant. When α is less than two the solid-liquid interface is atomically rough and exhibits non-faceted growth. The value of Jackson's roughness parameter (α) is given in Table 1. For the entire solid dispersions the α value was found greater than 2 which indicate the faceted [26] growth proceeds in all the cases.

**Table 1: Phase composition, melting temperature, values of entropy of fusion per unit volume ($\Delta S_v$), heat of fusion(ΔH), interfacial energy(σ), grain boundary energy($\sigma_{gb}$), Gibbs-Thomson coefficient (τ) and roughness parameter(α)**

| Alloy | $\chi_{PT}$ | MP | ΔH (J/mol) | ΔS (J/mol/K) | α | $\sigma \times 10^2$ ($J/m^2$) | $\sigma_{gb} \times 10^2$ ($J/m^2$) | $\Delta S_v$ ( $kJ/m^3/K$) | $\Delta H_v$ | $\tau \times 10^6$ Km |
|---|---|---|---|---|---|---|---|---|---|---|
| A1 | 0.044 | 141 | 13238.82 | 31.98 | 3.85 | 2.66 | 5.14 | 373.12 | 154.47 | 7.13 |
| A2 | 0.093 | 136 | 13882.34 | 33.94 | 4.08 | 2.72 | 5.26 | 382.04 | 156.25 | 7.13 |
| A3 | 0.150 | 133 | 14619.50 | 36.01 | 4.33 | 2.79 | 5.40 | 389.53 | 158.15 | 7.17 |
| A4 | 0.182 | 127 | 15028.16 | 37.57 | 4.52 | 2.83 | 5.47 | 397.85 | 159.14 | 7.12 |
| E | 0.215 | 122 | 15468.76 | 39.16 | 4.71 | 2.87 | 5.55 | 405.46 | 160.16 | 7.08 |
| A5 | 0.252 | 128 | 15944.69 | 39.76 | 4.78 | 2.91 | 5.63 | 402.02 | 161.21 | 7.25 |
| A6 | 0.292 | 140 | 16460.41 | 39.86 | 4.79 | 2.96 | 5.71 | 392.97 | 162.30 | 7.53 |
| A7 | 0.382 | 147 | 17631.61 | 41.98 | 5.05 | 3.05 | 5.90 | 391.84 | 164.57 | 7.79 |
| A8 | 0.490 | 159 | 19037.22 | 44.07 | 5.30 | 3.16 | 6.11 | 386.58 | 167.00 | 8.19 |
| A9 | 0.622 | 162 | 20754.47 | 47.71 | 5.74 | 3.29 | 6.36 | 389.89 | 169.60 | 8.44 |
| A10 | 0.788 | 174 | 22900.70 | 51.23 | 6.16 | 3.44 | 6.64 | 385.65 | 172.39 | 8.91 |
| PHZ | | 189 | 25660.00 | 55.54 | 6.68 | 3.61 | 6.98 | 379.62 | 175.38 | 9.51 |
| MIZ | | 142 | 12670.00 | 30.53 | 3.67 | 2.60 | 5.03 | 368.15 | 152.78 | 7.07 |

**Table 2: Value of partial and integral mixing of Gibbs free energy($\Delta G^M$), enthalpy($\Delta H^M$) and entropy($\Delta S^M$) of PT - MIM system**

| Alloy | $\Delta G_{PT}^{-M}$ J/mol | $\Delta G_{MIM}^{-M}$ J/mol | $\Delta G^M$ J/mol | $\Delta H_{PT}^{-M}$ J/mol | $\Delta H_{MIM}^{-M}$ J/mol | $\Delta H^M$ J/mol | $\Delta S_{PT}^{-M}$ J/mol/K | $\Delta S_{MIM}^{-M}$ J/mol/K | $\Delta S^M$ J/mol/K |
|---|---|---|---|---|---|---|---|---|---|
| A1 | -2665.97 | -30.53 | -145.93 | 8101.85 | 123.59 | 11667.44 | 26.01 | 0.37 | 1.49 |
| A2 | -2943.68 | -183.18 | -440.81 | 5120.88 | 149.98 | 8671.28 | 19.72 | 0.81 | 2.58 |
| A3 | -3110.30 | -274.77 | -700.32 | 3291.66 | 274.12 | 6941.26 | 15.77 | 1.35 | 3.52 |
| A4 | -3443.55 | -457.95 | -999.95 | 2230.92 | 208.25 | 5764.77 | 14.19 | 1.67 | 3.94 |
| E | -3721.26 | -610.60 | -1280.81 | 1319.74 | 186.27 | 4790.04 | 12.76 | 2.02 | 4.33 |
| A5 | -3388.01 | -427.42 | -1173.77 | 1205.98 | 541.00 | 5080.90 | 11.46 | 2.42 | 4.69 |
| A6 | -2721.52 | -61.06 | -837.37 | 1507.77 | 1123.63 | 6065.08 | 10.24 | 2.87 | 5.02 |
| A7 | -2332.73 | 152.65 | -796.66 | 1028.03 | 1832.93 | 6352.84 | 8.00 | 4.00 | 5.53 |
| A8 | -1666.23 | 519.01 | -552.12 | 894.67 | 2938.58 | 7424.90 | 5.93 | 5.60 | 5.76 |
| A9 | -1499.61 | 610.60 | -702.71 | 215.50 | 4132.49 | 7964.59 | 3.94 | 8.10 | 5.51 |
| A10 | -833.12 | 976.96 | -448.62 | 54.30 | 6734.36 | 10505.02 | 1.99 | 12.88 | 4.30 |

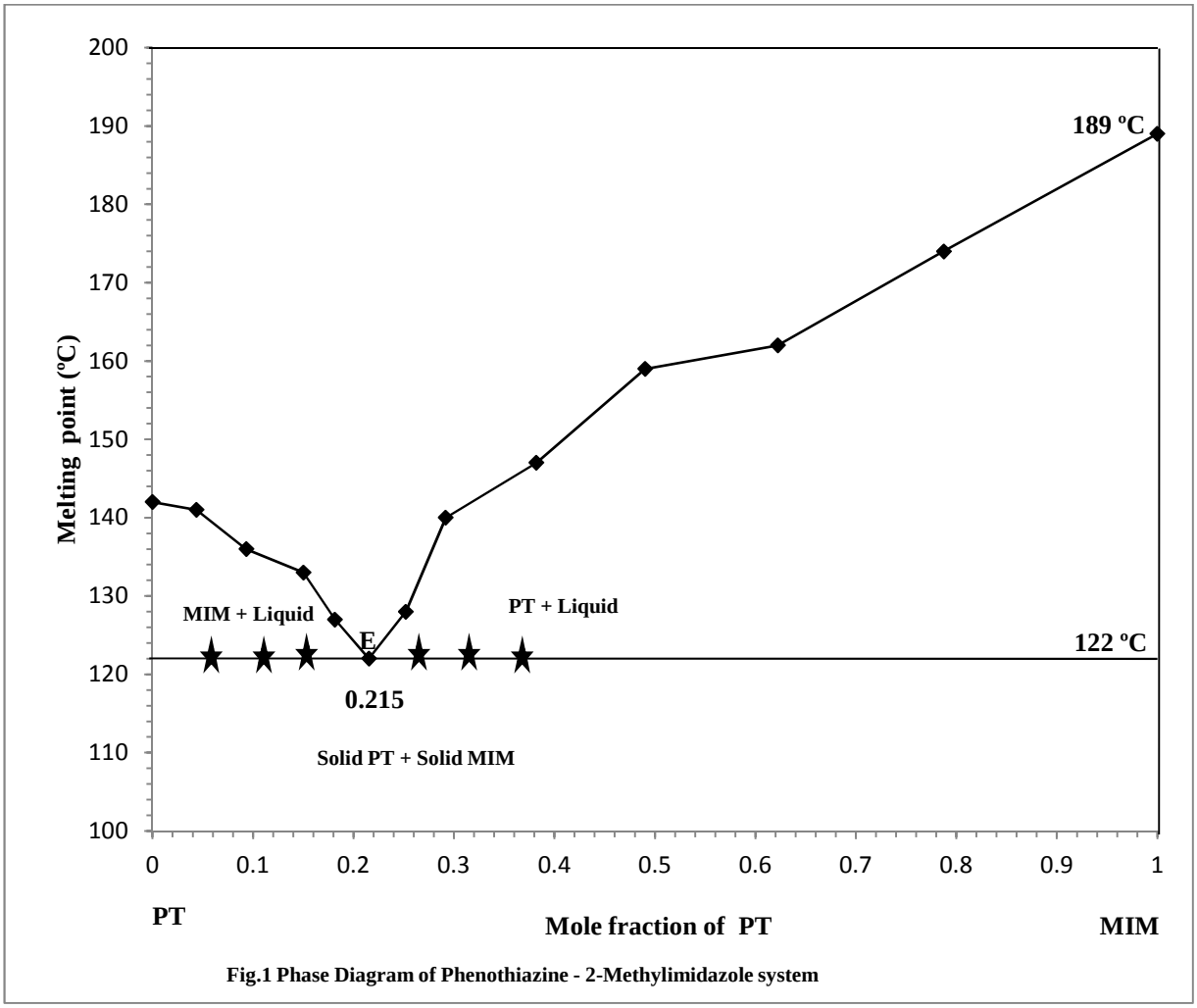


**Fig.1 Phase Diagram of Phenothiazine - 2-Methylimidazole system**

**Table 3: Value of partial and integral excess Gibbs free energy($g^E$), enthalpy($h^E$) and entropy($s^E$) of PT - MIM system**

| Alloy | $g_{PT}^{-E}$ J/mol | $g_{MIM}^{-E}$ J/mol | $g^E$ J/mol | $h_{PT}^{-E}$ J/mol | $H_{MIM}^{-E}$ J/mol | $h^E$ J/mol | $s_{PT}^{-E}$ J/mol/K | $s_{MIM}^{-E}$ J/mol/K | $s^E$ J/mol/K |
|---|---|---|---|---|---|---|---|---|---|
| A1 | 8101.85 | 123.59 | 472.95 | 625178.38 | 17134.86 | 43760.63 | 1490.52 | 41.09 | 104.56 |
| A2 | 5120.88 | 149.98 | 613.90 | 123359.45 | 2669.34 | 13933.15 | 289.09 | 6.16 | 32.57 |
| A3 | 3291.66 | 274.12 | 726.98 | 19998.03 | -4607.82 | -915.04 | 41.15 | -12.02 | -4.04 |
| A4 | 2230.92 | 208.25 | 575.44 | 10978.42 | -4543.56 | -1725.76 | 21.87 | -11.88 | -5.75 |
| E | 1319.74 | 186.27 | 430.48 | 94754.05 | 20398.65 | 36418.91 | 236.54 | 51.17 | 91.11 |
| A5 | 1205.98 | 541.00 | 708.64 | 855.96 | -3732.39 | -2575.70 | -0.87 | -10.66 | -8.19 |
| A6 | 1507.77 | 1123.63 | 1235.72 | 22939.62 | 7354.00 | 11901.80 | 51.89 | 15.09 | 25.83 |
| A7 | 1028.03 | 1832.93 | 1525.49 | 51133.57 | 34789.09 | 41031.97 | 119.30 | 78.47 | 94.06 |
| A8 | 894.67 | 2938.58 | 1936.73 | 37649.19 | 48196.23 | 43026.46 | 85.08 | 104.76 | 95.12 |
| A9 | 215.50 | 4132.49 | 1694.71 | 24896.43 | 70648.48 | 42174.20 | 56.74 | 152.91 | 93.06 |
| A10 | 54.30 | 6734.36 | 1473.26 | 5978.81 | 104637.76 | 26935.66 | 13.25 | 219.02 | 56.96 |

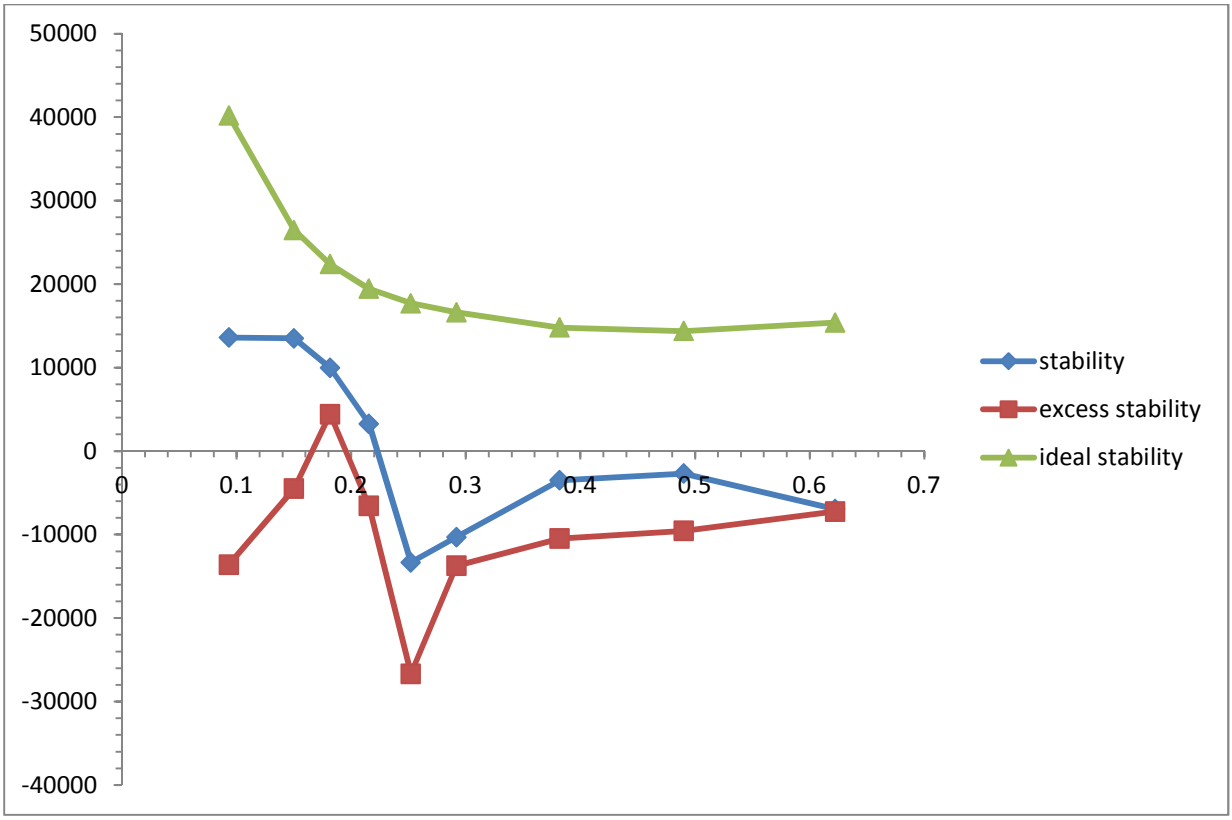


**Fig.2. Stability Graph of PT-MIM System**

**Table 4: Value of volume free energy change ($\Delta G_v$) during solidification for PT - MIM system of different undercoolings ($\Delta T$)**

| Alloy ↓ ΔT | $\Delta G_v$(J/cm$^3$) | | | | | |
|---|---|---|---|---|---|---|
| | **1.0→** | **1.5** | **2.0** | **2.5** | **3.0** | **3.5** |
| A1 | 0.37 | 0.56 | 0.75 | 0.93 | 1.12 | 1.31 |
| A2 | 0.38 | 0.57 | 0.76 | 0.96 | 1.15 | 1.34 |
| A3 | 0.39 | 0.58 | 0.78 | 0.97 | 1.17 | 1.36 |
| A4 | 0.40 | 0.60 | 0.80 | 0.99 | 1.19 | 1.39 |
| E | 0.41 | 0.61 | 0.81 | 1.01 | 1.22 | 1.42 |
| A5 | 0.40 | 0.60 | 0.80 | 1.01 | 1.21 | 1.41 |
| A6 | 0.39 | 0.59 | 0.79 | 0.98 | 1.18 | 1.38 |
| A7 | 0.39 | 0.59 | 0.78 | 0.98 | 1.18 | 1.37 |
| A8 | 0.39 | 0.58 | 0.77 | 0.97 | 1.16 | 1.35 |
| A9 | 0.39 | 0.58 | 0.78 | 0.97 | 1.17 | 1.36 |
| A10 | 0.39 | 0.58 | 0.77 | 0.96 | 1.16 | 1.35 |
| PHZ | 0.38 | 0.57 | 0.76 | 0.95 | 1.14 | 1.33 |
| MIZ | 0.37 | 0.55 | 0.74 | 0.92 | 1.10 | 1.29 |

**Table 5: Critical size of nucleus (r*) at different undercoolings ($\Delta T$)**

| Alloy → ΔT ↓ | r*(nm) | | | | | |
|---|---|---|---|---|---|---|
| | **1.0** | **1.5** | **2.0** | **2.5** | **3.0** | **3.5** |
| A1 | 142.65 | 95.101 | 71.33 | 57.06 | 47.55 | 40.76 |
| A2 | 142.63 | 95.086 | 71.31 | 57.05 | 47.54 | 40.75 |
| A3 | 143.47 | 95.645 | 71.73 | 57.39 | 47.82 | 40.99 |
| A4 | 142.36 | 94.904 | 71.18 | 56.94 | 47.45 | 40.67 |
| E | 141.64 | 94.424 | 70.82 | 56.65 | 47.21 | 40.47 |
| A5 | 144.93 | 96.620 | 72.47 | 57.97 | 48.31 | 41.41 |
| A6 | 150.52 | 100.35 | 75.26 | 60.21 | 50.17 | 43.01 |
| A7 | 155.90 | 103.93 | 77.95 | 62.36 | 51.97 | 44.54 |
| A8 | 163.70 | 109.13 | 81.85 | 65.48 | 54.57 | 46.77 |
| A9 | 168.78 | 112.52 | 84.39 | 67.51 | 56.26 | 48.22 |
| A10 | 178.25 | 118.83 | 89.12 | 71.30 | 59.42 | 50.93 |
| PHZ | 190.26 | 126.84 | 95.13 | 76.10 | 63.42 | 54.36 |
| MIZ | 141.44 | 94.290 | 70.720 | 56.57 | 47.15 | 40.41 |

**Table 6: Value of critical free energy of nucleation (ΔG*) for alloys of PT - MIM system at different undercooling (ΔT)**

| Alloy → / ΔT ↓ | ΔG*×10$^{16}$ (J) | | | | | |
|---|---|---|---|---|---|---|
| | **1.0** | **1.5** | **2.0** | **2.5** | **3.0** | **3.5** |
| A1 | 22.69 | 10.09 | 5.67 | 3.63 | 2.52 | 1.85 |
| A2 | 23.23 | 10.32 | 5.81 | 3.72 | 2.58 | 1.90 |
| A3 | 24.10 | 10.71 | 6.03 | 3.86 | 2.68 | 1.97 |
| A4 | 24.05 | 10.69 | 6.01 | 3.85 | 2.67 | 1.96 |
| E | 24.14 | 10.73 | 6.04 | 3.86 | 2.68 | 1.97 |
| A5 | 25.64 | 11.40 | 6.41 | 4.10 | 2.85 | 2.09 |
| A6 | 28.08 | 12.48 | 7.02 | 4.49 | 3.12 | 2.29 |
| A7 | 31.11 | 13.82 | 7.78 | 4.98 | 3.46 | 2.54 |
| A8 | 35.53 | 15.79 | 8.88 | 5.69 | 3.95 | 2.90 |
| A9 | 39.28 | 17.46 | 9.82 | 6.28 | 4.36 | 3.21 |
| A10 | 45.76 | 20.34 | 11.44 | 7.32 | 5.08 | 3.74 |
| PHZ | 54.78 | 24.35 | 13.69 | 8.76 | 6.09 | 4.47 |
| MIZ | 21.82 | 9.70 | 5.46 | 3.49 | 2.42 | 1.78 |

## CONCLUSION

The solid-liquid equilibrium phase diagram of PT-MIM system shows the formation of simple eutectic alloy. The activity and activity coefficient values are very useful in computing thermodynamic mixing and excess functions. Thermodynamic excess and mixing functions $g^E$ and $\Delta G^M$ values for eutectic and non-eutectic dispersions are being found positive and negative respectively which suggest the stronger association between like molecules and there is spontaneous mixing in all the binary drugs.

**Acknowledgement**
Thanks are due to the Head Department of Chemistry, V K S University Ara 802301, India for providing research facilities.

## REFERENCES

[1] Spengler, G.; handzlik, J.; Oscovszki, I.; Viveiros, M.; Kiec-Kononowicz, K.; Molnar, J.; Amaral, L., *Anticancer Res.*, **2011**, 31(10), 3285-3288.
[2] Urszula Domanska, Aleksandra Pelczarska, Aneta Pobudkowska, *International Journal of Pharmaceutics*, **2011**, 421(1), 135-144.
[3] Ritu Sharma, Pushkal Samadhiya, S. D. Srivastava and S. K. Srivastava, *J. Chem. Sci.*, **2012**, 124(3), 633-637.
[4] CHEN Bin-Yuan, ZHANG Xue-Sheng and LI Ding-Long, *Chinese J. Struct. Chem.*, **2011,** 30(11), 1575-1584.
[5] Sabatini, S., Kaatz, G.W., Rossolini, G.M., Brandini, D. Fravolini, A., *J. Med. Chem.*, **2008**, 51(14), 4321-30.
[6] A.G. Martinez, T. Montoro, M.H. vinas and G. Tardajos., *J. Pharm. Sci.*, **2008**, 97(4), 1484-1498.
[7] The Merck Index, *An Encyclopedia of Chemicals, drugs and Biologicals, 13th edition, merck Resarch lab*, 2001.
[8] Ansari KF, Lal C., *J. Chem. Sci.*, **2009**, 121(16), 1017-1025.
[9] Kazimierczuk Z., Upcroft J. A., Upcroft P., Gorska A., Starosciak B., and Agnieszka L., *Acta Biochemica Polonica*, **2002**, 49(1), 185-195.
[10] Michele Tonelli et.al., *Bioorganic & Medicinal Chemistry*, **2010**, 18, 2937-2953.
[11] Sangster, J., *J. Phy. Chem. Ref. Data*, **1999**, 28, 889-930.
[12] Sharma, B. L., Tandon, S., & Gupta S., *Cryst. Res. Technol.*, **2009**, 44, 258-268.
[13] Malaviolle, R., et al., *Thermochemi. Acta*, **1988**, 121, 283.
[14] Shekhar, H. and Salim, S. S., *J. Nat. Acad. Sci Letter*, **2011**, 34, 117-125.
[15] Nieto, R., Gonozalez, M. C., & Herrero, F., *American Journal of Physics*, **1999**, 67, 1096-1099.
[16] Agrwal, T., et al., *J. Chem. Engg. Data*, **2010**, 55, 4206-4210.
[17] Shekhar H and Kant Vishnu, *Asian Journal of Chemistry*, **2013**, 25 (5), 2441-2446.
[18] Singh, N. B., Glicksman, M. E., *J. Cryst. Growth*, **1989**, 98, 573-580.
[19] Shekhar H and Vishnu Kant, *Molecular Crystal Liquid Crystal*, **2013**, 577(1) 103-115
[20] Gunduz, M., & Hunt. J. D., *Acta Metall.*, **1989**, 37, 1839.
[21] Akbulut, S., Ocak, Y., Keslioglu, K., & Marasli, N., *Applied Surface Science*, **2009**, 255, 3594-3599.
[22] Hunt, J. D., & Lu, S. Z., *Hand Book of Crystal Growth Ed. DTJ Hurle, Elsevier, Amsterdam*, **1994**, 112
[23] Chadwick, G. A., *Metallography of Phase Transformation, Butterworths, London*, **1972**, 61
[24] Kant Vishnu and Shekhar H, *Bulgarian Journal of Science Education*, **2014**, 23(2), 232-247.
[25] Hunt, J. D., & Jackson, K. A., *Trans. Metall. Soc. AIME*, **1966**, 236, 843.
Shekhar, H., & Kant, V., *I. J. Chem. Soc.*, **2011**, 88, 947-952.